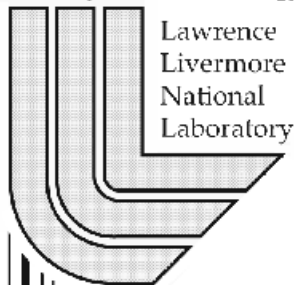


FitzHugh-Nagumo Revisited: Types of Bifurcations, Periodical Forcing and Stability Regions by a Lyapunov Functional

*Tanya Kostova
Renuka Ravindran and Maria Schonbek*

This article was submitted to International Journal of Bifurcation and Chaos

U.S. Department of Energy



Lawrence
Livermore
National
Laboratory

February 6, 2003

DISCLAIMER

This document was prepared as an account of work sponsored by an agency of the United States Government. Neither the United States Government nor the University of California nor any of their employees, makes any warranty, express or implied, or assumes any legal liability or responsibility for the accuracy, completeness, or usefulness of any information, apparatus, product, or process disclosed, or represents that its use would not infringe privately owned rights. Reference herein to any specific commercial product, process, or service by trade name, trademark, manufacturer, or otherwise, does not necessarily constitute or imply its endorsement, recommendation, or favoring by the United States Government or the University of California. The views and opinions of authors expressed herein do not necessarily state or reflect those of the United States Government or the University of California, and shall not be used for advertising or product endorsement purposes.

This is a preprint of a paper intended for publication in a journal or proceedings. Since changes may be made before publication, this preprint is made available with the understanding that it will not be cited or reproduced without the permission of the author.

This research was supported under the auspices of the U.S. Department of Energy by the University of California, Lawrence Livermore National Laboratory under contract No. W-7405-Eng-48.

FitzHugh-Nagumo Revisited: Types of Bifurcations, Periodical Forcing and Stability Regions by a Lyapunov Functional

Tanya Kostova
Lawrence Livermore National Laboratory
L-561, Livermore, CA 94550, USA
E-mail: kostova@llnl.gov

Renuka Ravindran
Department of Mathematics,
Indian Institute of Science,
Bangalore 560012 India

Maria Schonbek
Department of Mathematics,
University of California at Santa Cruz,
Santa Cruz, CA 95064 USA

December 19, 2003

AMS Subject Classification: 34D, 37N, 65P

Running Head : FitzHugh-Nagumo Revisited

Author to whom correspondence should be sent:
Tanya Kostova
L-561 Lawrence Livermore National Laboratory
7000 East Avenue,
Livermore, CA 94550, USA
E-mail adress: kostova@llnl.gov

Abstract

We study several aspects of FitzHugh-Nagumo's (FH-N) equations without diffusion. Some global stability results as well as the boundedness of solutions are derived by using a suitably defined Lyapunov functional. We show the existence of both supercritical and subcritical Hopf bifurcations. We demonstrate that the number of all bifurcation diagrams is 8 but that the possible sequential occurrences of bifurcation events is much richer. We present a numerical study of an example exhibiting a series of various bifurcations, including subcritical Hopf bifurcations, homoclinic bifurcations and saddle-node bifurcations of equilibria and of periodic solutions. Finally, we study periodically forced FH-N equations. We prove that phase-locking occurs independently of the magnitude of the periodic forcing.

Keywords: *FitzHugh-Nagumo, subcritical and supercritical Hopf bifurcation, homoclinic bifurcation, periodic forcing*

1 Introduction

We consider the FitzHugh-Nagumo (FH-N) equations without diffusion,

$$\begin{aligned}\frac{du}{dt} &= \varepsilon g(u) - w + I, \\ \frac{dw}{dt} &= u - aw,\end{aligned}\tag{1.1}$$

where $g(u) = u(u - \lambda)(1 - u)$, $0 < \lambda < 1$ and $a, \varepsilon > 0$. We remark that in the existing literature, the term "FitzHugh-Nagumo system" has been used to refer to both the models with and without diffusion.

Although equations (1.1) have been mentioned in practically every mathematical biology book [2], [8], [12], as well as some of their aspects have been studied in different contexts, [1, 4, 9, 10, 11] there is no detailed treatment of their dynamics from the point of view of nonlinear dynamics theory.

Our goal in writing the present paper has been to offer a detailed analysis of the FH-N system (1.1) and to present a theoretical proof of phase-locking of coupled FH-N oscillators.

We demonstrate that the system exhibits many of the known bifurcation types, some of which are executed in a non-typical way.

In various cases the FH-N system possesses unstable periodic solutions, which appear via subcritical Hopf bifurcations. (The instability is probably the reason for which such solutions were not noticed in [8], p.164.) In other cases, supercritical Hopf bifurcations occur. The Bogdanov-Takens bifurcation [7] is also characteristic for this system. As noted below, homoclinic bifurcations and saddle-node bifurcations of equilibria and of periodic solutions are also exhibited by this system.

It is a common practice to represent a dynamical system by its bifurcation diagram. We show that the possible bifurcation diagrams for the FH-N equation are 8. However, because of the possibilities of occurrence of both supercritical and subcritical Hopf bifurcations, as well as the occurrence of homoclinic orbits of the saddle associated with the appearance/disappearance of periodic orbits, the number of possible sequences of bifurcation events is much larger. Thus a bifurcation diagram is not always sufficiently informative about the system.

As evidence, we present an example which possesses a richness of bifurcation events when the parameter I is varied. The numerical experiments with the example show a sudden disappearance of two (stable and unstable) periodic orbits, which seems to occur simultaneously near a certain value of I . A more careful numerical investigation uncovers that the stable and unstable periodic orbits appear and disappear via different bifurcations associated with the homoclinic orbits of the saddle. The careful study of the mentioned example shows that besides saddle-node bifurcations of equilibria and subcritical Hopf bifurcations, the FitzHugh - Nagumo system exhibits also saddle-node bifurcations of periodic orbits and homoclinic bifurcations which occur in a very narrow interval (of the magnitude of 10^{-7} of values of I). In-between, the structurally unstable homoclinic orbit of the saddle converts into a heteroclinic orbit connecting the saddle and the unstable equilibrium which further converts back into a homoclinic orbit of the saddle.

In short, from the standpoint of a "bifurcation gems collector", the well-known, simple-looking system (1.1) is a treasure box which, we believe, is worthwhile opening once more.

The structure of the paper is as follows.

In Section 2 we introduce a Lyapunov functional for the system, which is of help in establishing various useful results. We use it to state global stability results for certain sets of parameter values and to prove the boundedness of the solutions of the system. In Section 3, we carry out the phase plane and bifurcation analysis of the system. In Section 4 we study the case when I is not a constant. Since a system of the type (1.1) represents an oscillator (as in many cases it possesses a limit cycle), an interesting problem is to study periodically forced FH-N equations. Results from [5] are used to prove the existence of periodic solutions with the same period as the forcing term. We note that our result predicts the occurrence of phase-locking, regardless of the amplitude of the forcing term.

2 Stability and boundedness via a Lyapunov functional

2.1 Existence and linear stability of equilibrium points

Depending on the parameters, system (1.1) can have one, two or three equilibrium points. At least one equilibrium always exists and the number of equilibria cannot be more than three.

Let $b_1 = g'(u_e)$. It is trivial to establish (noticing that b is a function of a):

Proposition 2.1. *Let (u_e, w_e) be an equilibrium point. Let $\varepsilon ab_1 < 1$, then (u_e, w_e) is locally asymptotically stable if $\varepsilon b_1 < a$ and is a repeller if $\varepsilon b_1 > a$. If $\varepsilon ab_1 > 1$, then (u_e, w_e) is a saddle point. If $\varepsilon ab_1 = 1$, then (u_e, w_e) is unstable if $\varepsilon b_1 > a$.*

2.2 A Lyapunov Functional for FitzHugh-Nagumo's Equations

We introduce the values

$$T = (1 - \varepsilon b_1 a) - \frac{2\varepsilon ab_2^2}{9}$$

and

$$S = \frac{b_2^2}{3} + b_1 - \frac{a}{\varepsilon}$$

where $b_1 = g'(u_e)$ and $b_2 = g''(u_e)/2$.

Proposition 2.2. *Let (u_e, w_e) be an equilibrium of (1.1). Let*

$$V(u, w) = \frac{1}{2}[u - u_e - a(w - w_e)]^2 + G(w - w_e), \quad (2.1)$$

where $G(x) = \frac{1}{4}\varepsilon ax^2[a^2x^2 - \frac{4}{3}axb_2 - 2(b_1 - \frac{1}{a\varepsilon})]$.

Let the line L be defined by $L = \{(u, w) | u = u_e + a(w - w_e)\}$. Then,

a) $V(u, w) > 0$ for all $(u, w) \neq (u_e, w_e)$ if and only if $T > 0$. If $T \leq 0$, then $V \leq 0$ in a bounded set S , which is symmetric about the line L .

b) On L the derivative $\dot{V} \equiv \frac{\partial V}{\partial u}\dot{u} + \frac{\partial V}{\partial w}\dot{w} = 0$. Additionally, $\dot{V} < 0$ iff $S < 0$ and $(u, w) \notin L$. If $S \geq 0$, there exists an ellipse $\partial\mathcal{E}$, surrounding a region \mathcal{E} such that: i) $\dot{V} < 0$ if (u, w) belongs to the complement of $\partial\mathcal{E} \cup \mathcal{E} \cup L$; ii) $\dot{V} > 0$ if $(u, w) \in \mathcal{E} \setminus (L \cap \mathcal{E})$.

c) If $\varepsilon b_1 a < 1$ and $\varepsilon b_1 > a$, there exists a neighborhood of the equilibrium (u_e, w_e) which no solution enters. If $\varepsilon b_1 a < 1$ and $b_1 \varepsilon < a$, there is a neighborhood of the equilibrium which no solution leaves. These neighborhoods can be found explicitly by using level curves of V .

d) Suppose $T > 0$ and $S < 0$. If (u_e, w_e) is unique, it is globally asymptotically stable. If (u_e, w_e) is not unique, it is the only stable equilibrium.

Proof. After the transformations $v = u - u_e$, $s = w - w_e$, and $v - as = y$, $s = x$ the system can be rewritten as

$$\dot{x}(t) = y \quad \dot{y}(t) = -yf(x, y) - g_1(x),$$

where

$$f(x, y) = \varepsilon(y^2 + (3ax - b_2)y + (3a^2x^2 - 2b_2ax - b_1)) + a,$$

$$g_1(x) = -\varepsilon(b_1ax + b_2a^2x^2 - a^3x^3) + x.$$

The line L is the one with equation $y = 0$.

Then

$$V(x, y) = y^2/2 + G(x),$$

and

$$G(x) = \int_0^x g_1(\xi) d\xi. \quad (2.2)$$

A simple computation yields that $G(x) > 0 \forall x \neq 0$ (and therefore $V(x, y) > 0, \forall (x, y) \neq (0, 0)$) if and only if $T > 0$. The level curves $V(x, y) = c, c > 0$ are closed nested ovals encircling the origin.

If $T < 0$, the set $V(x, y) = 0$ consists of $(0, 0)$ and a closed curve, defined by

$$y^2 = \frac{1}{2}\varepsilon ax^2 \left[-a^2 x^2 + \frac{4}{3}ab_2 x + 2\left(b_1 - \frac{1}{\varepsilon a}\right) \right]. \quad (2.3)$$

If $T = 0$, the set $V(x, y) = 0$ consists of $(0, 0)$ and another point on the $y = 0$ axis.

It is symmetric about the axis $y = 0$ and surrounds a bounded set \mathcal{S} such that $V(x, y) \leq 0$ if $(x, y) \in \mathcal{S}$.

b) $\dot{V}(x, y) = -y^2 f(x, y)$ and obviously $\dot{V} = 0$ on L and $\dot{V} < 0$ iff $f(x, y) > 0$ and $y \neq 0$. The last is true for all (x, y) iff $S < 0$ which is calculated by transforming $f(x, y)$ into a quadratic form and analyzing it.

Alternatively, the curve $f(x, y) = 0$ is an ellipse \mathcal{E} in the (x, y) -plane if and only if $S > 0$. $\dot{V} > 0$ only in the interior of the ellipse excluding its intersection with L .

c) That the mentioned neighborhoods exist follows from Proposition 2.1. Next we clarify the construction of the level curves.

If $\varepsilon ab_1 < 1$ then there exists a neighborhood of $(0, 0)$ such that $V(x, y) > 0$ for all $(x, y) \neq (0, 0)$ in this neighborhood. I.e. if \mathcal{S} exists, it does not contain the origin. If also $\varepsilon b_1 > a$, then $S > 0$. Therefore $\dot{V} > 0$ inside \mathcal{E} (which exists according to b)) except on $L \cap \mathcal{E}$. \mathcal{E} surrounds the origin because $f(0, 0) = -\varepsilon b_1 + a$, i.e. $\dot{V} > 0$ in the vicinity of the origin (except on the line $y = 0$). It is then enough to find a level curve $V = c$ which is outside of \mathcal{S} (if it exists) and inside \mathcal{E} to ensure that the trajectories of all solutions starting on the curve do not enter the region surrounded by it.

Alternatively, if $\varepsilon b_1 < a$, the ellipse \mathcal{E} either does not exist or does (provided $S > 0$) but the origin lies outside it. Then the level curve we are looking for is one that does not cross both \mathcal{S} and \mathcal{E} .

d) If $T > 0$ and $S < 0$, then $V > 0$ and $\dot{V} \leq 0$ (with $\dot{V} = 0$ only on $y = 0$). Since V is monotone decreasing along the trajectory of any non-equilibrium solution and bounded below, the solution must converge to a point $(x^*, 0)$ and the only such point is the equilibrium.

If (u_e, w_e) is not unique, let (u_*, w_*) be any other equilibrium. Take the region surrounded by the level curve $V(x, y) = V(u_* - u_e, w_* - w_e) - \delta$ for arbitrarily small $\delta > 0$. All solutions starting in this region converge to an equilibrium contained in the region, which is either (u_e, w_e) or at most another one (the third) equilibrium. Because δ is arbitrarily small, (u_*, w_*) cannot be stable.

Finally, to obtain the statements of the proposition, we return back to coordinates u, w .

2.3 Boundedness of the Solutions

The Lyapunov functional allows to prove the boundedness of solutions of (1.1) in an elegant way.

Proposition 2.3. *There exists a family of nested bounded forward invariant sets of (1.1) covering the whole (u, w) -plane. Thus, every solution of (1.1) is bounded for $t > 0$.*

Proof. Consider the functional V defined by (2.1). Let \mathcal{S} and \mathcal{E} be the regions from the previous section, if they exist.

Since \mathcal{E}, \mathcal{S} are bounded sets, we choose $\bar{c} = \min\{c \geq 0 \mid V(u, w) = c \supset \mathcal{E} \cup \mathcal{S} \cup (u_e, w_e)\}$. Then for any sequence

$$\{c_i\}, c_i > c_{i-1} > \dots \bar{c}, c_i \rightarrow \infty, i \rightarrow \infty,$$

the curves $V(u, w) = c_i$ enclose nested bounded sets D_i such that any point (u, w) belongs to such a set for a sufficiently large c_i . Each of the sets D_i is a forward invariant set. Thus, each solution of (1.1) is bounded and confined in a forward invariant set containing its initial condition.

3 Phase plane and bifurcation analysis

The possible phase plane portraits of the system (1.1) were revealed in [1]. Here we are interested in *how* such portraits can appear, the types of bifurcations, the values of the parameters when changes arise.

Proposition 3.1. *As the eigenvalues μ_1, μ_2 of any equilibrium (u_e, w_e) are of the form*

$$\mu_{1,2} = \frac{1}{2}R(\varepsilon, a, b_1) \pm \frac{1}{2}\sqrt{R^2 + 4Q}, \quad (3.1)$$

where $Q(\varepsilon, a, b_1) \equiv \varepsilon ab_1 - 1$ and $R \equiv \varepsilon b_1 - a$, Hopf bifurcation occurs in cases when $R = 0$ and $Q < 0$.

3.1 The case with $I = 0$

We consider this case separately because the equilibria can be found explicitly.

In this case $(u_e, w_e) = (0, 0)$ is always an equilibrium point. Then $b_1 \equiv g'(u_e) = -\lambda < 0$, and according to Proposition 2.1, it is always locally stable.

3.1.1. Single Equilibrium Point.

First, $(0, 0)$ is the only equilibrium point if and only if

$$1 - \frac{4}{\varepsilon a(1-\lambda)^2} < 0. \quad (3.2)$$

Proposition 3.2. *Let $I = 0$, suppose $(0, 0)$ is a unique equilibrium point. Suppose*

$$a > \frac{1}{4}\varepsilon \quad \text{and} \quad (3.3)$$

$$\frac{1}{2} - \sqrt{3\left(\frac{a}{\varepsilon} - \frac{1}{4}\right)} < (1-\lambda) < \frac{1}{2} + \sqrt{3\left(\frac{a}{\varepsilon} - \frac{1}{4}\right)}$$

holds, then the equilibrium point $(0, 0)$ is globally asymptotically stable.

The proof uses the Lyapunov functional and is in Appendix A.

For the case when (3.3) does not hold, one can only state

Proposition 3.3. *Let $(0, 0)$ be a unique equilibrium point. If (3.3) does not hold, $(0, 0)$ is either globally asymptotically stable, or there exists a stable periodic orbit.*

The proof follows from Poincare- Bendixon's theorem. However, we have not been able to observe an instance when such an orbit exists for the case of unique equilibrium.

As $(0, 0)$ is always stable, Hopf bifurcations do not occur in this case.

3.1.2. More Than One Equilibrium: Subcritical Hopf and Bogdanov-Takens Bifurcation

On the two-dimensional parameter surface $\varepsilon a(1-\lambda)^2 = 4$ a saddle-node bifurcation of equilibria occurs. Bogdanov-Takens (B-T) bifurcations [7] occur when $a = 1$ and $\varepsilon a(1-\lambda)^2 = 4$. Small limit cycles exist in the vicinity of the curve $a = 1, \varepsilon = \frac{4}{(1-\lambda)^2}$ at least for $a < 1$. Here we describe in some detail how the B-T bifurcation is accomplished.

If $\varepsilon a(1-\lambda)^2 > 4$, there are 2 equilibrium points in the first quadrant, $E_1 = (u_1, w_1)$ and $E_2 = (u_2, w_2)$, where

$$u_1 = p - r\sqrt{q}, \quad u_2 = p + r\sqrt{q} \quad w_i = \frac{u_i}{a} \quad \text{and} \quad (3.4)$$

$$q = 1 - \frac{4}{\varepsilon a(1-\lambda)^2}, \quad p = \frac{1+\lambda}{2}, \quad r = \frac{1-\lambda}{2}.$$

At E_1 , $\varepsilon a b_1 > 1$, which, according to Proposition 2.1 implies that E_1 is always a saddle point.

It is easy to check that for $E_2, b_1 = \frac{1}{a\varepsilon} - (1-\lambda)\sqrt{q}u_2$. Then $Q < 0$ and it follows that E_2 is stable if $R < 0$, a repeller if $R > 0$ and undergoes Hopf bifurcation when $R = 0$. The type of the Hopf bifurcation (super or subcritical) cannot be determined in general, but in particular, for each given set of values of the parameters calculations to determine it can be carried out, as done in Appendix B.

More precisely, if $\varepsilon a(1-\lambda)^2 > 4$, the equilibrium E_2 is unstable if

$$aR \equiv 1 - a^2 - \varepsilon a(1-\lambda)\sqrt{q}\left[\frac{1+\lambda}{2} + \frac{1-\lambda}{2}\sqrt{q}\right] > 0. \quad (3.5)$$

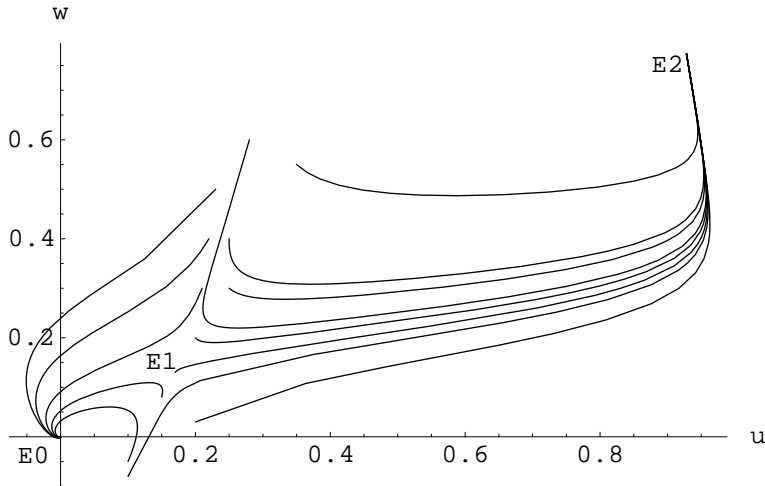


Figure 1: Phase plane trajectories in the (u, w) - plane, when both E_0, E_2 are stable. $I = 0$, $a = 1.2$, $\lambda = 0.1$, $\epsilon = 14$. $E_0 = (0, 0)$ and $E_2 = (0.928, 0.77)$.

We see from (3.5) that if $a \geq 1$, E_2 is stable independently of the values of ϵ, λ , because then $R < 0$ and $Q < 0$. Some trajectories are attracted by E_0 , others, by E_2 . Figure 1 shows a typical phase portrait in that case. The basins of attraction of both equilibria are separated by the stable manifold of the saddle E_1 .

If $a < 1$, E_2 is a repeller for sufficiently small values of q , i.e. near the surface $\epsilon a(1 - \lambda)^2 = 4$, immediately after the saddle-node bifurcation that causes the appearance of E_1 and E_2 .

For example, if $\epsilon = 14$, $a = 0.37$ and $\lambda = 0.1$, there are 2 positive equilibria besides the origin, and E_2 is a repeller, because (3.5) holds as is verified by direct calculation. All orbits, with the exception of the stable manifold of E_1 , are attracted to the origin.

Stated otherwise, if we fix $\epsilon > 4$ and consider the curve $a = \frac{4}{(1-\lambda)^2}$, for each $a < 1$ there is a value of λ (in fact an interval of values of λ) such that E_2 is a repeller. Starting from such values of a, ϵ, λ , while keeping $\epsilon > 4$ fixed and increasing a , since R is a decreasing function of a , R will eventually become negative and therefore E_2 will become stable. The exchange of stability is realized via Hopf bifurcation, because $Q < 0$. In the example above, by increasing a from 0.37, R becomes equal to 0 for $a \approx 0.379785$, which is the value of a for which Hopf bifurcation occurs. Numerical simulations show that the bifurcation is subcritical. An unstable periodic orbit exists for values of a larger than 0.379785, i.e. when E_2 is stable, as shown in Figure 2. Solutions, starting inside the unstable periodic orbit, approach E_2 , while solutions, starting outside of the unstable periodic orbit (with the exception of E_1 and its stable manifold), approach the other stable equilibrium $(0, 0)$ (Figure 2).

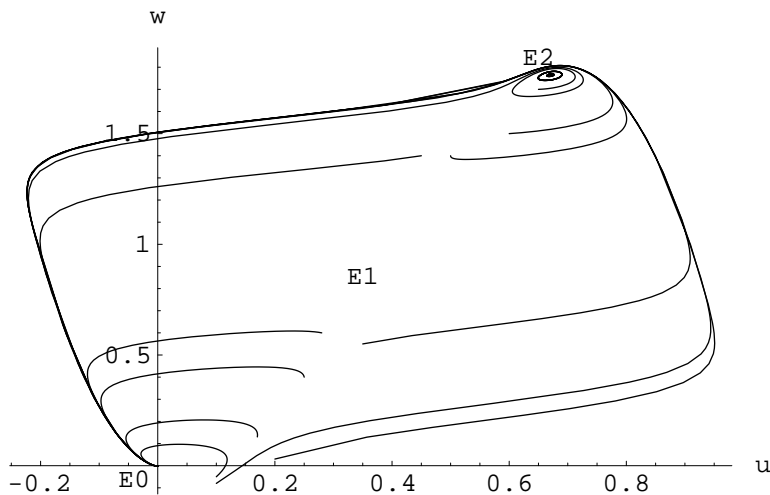


Figure 2: Phase plane trajectories in the (u, w) - plane, when both E_0, E_2 are stable, but an unstable periodic solution surrounds E_2 . All solutions starting near the orbit on its outer side approach E_0 . Solutions starting inside approach E_2 . $I = 0$, $a = 0.38$, $\lambda = 0.1$, $\epsilon = 14$.

That the Hopf bifurcation is subcritical can also be shown by direct calculation of the value G_4 (see Appendix B). The constant G_4 determining the type of the bifurcation is positive (22.5165), i.e. the bifurcation is subcritical.

The analyzed case illustrates a Bogdanov-Takens bifurcation, as when a passes through 1 at the intersection with the curve $a = \frac{4}{(1-\lambda)^2}$ for each fixed $\epsilon > 4$, both eigenvalues of the newly emerged equilibrium are 0. The Hopf bifurcation curve in the (a, λ) space passes through this intersection point.

We note that, when compared to the case delineated in [7], p. 281, our example is different in the order of events. In the case described in [7] the newly emerged equilibrium is stable and destabilizes while a stable periodic orbit appears. In our case, it is unstable near the bifurcation curve and stabilizes later with the appearance of an unstable periodic solution. Although this observation does not describe some completely new phenomenon, it is worthwhile mentioning from an educational point of view.

3.2 The case with $I \neq 0$

3.2.1. Existence of Equilibria

The equilibria in this case satisfy the equations

$$\begin{aligned} \epsilon g(u) - \frac{u}{a} + I &= 0, \quad I > 0, \\ w &= \frac{u}{a}. \end{aligned} \tag{3.6}$$

Here again, there might be one, two, or three equilibria. Let $\Phi(u) \equiv \epsilon g(u) - \frac{u}{a}$. An equilibrium (u_e, w_e) should satisfy the equation $\Phi(u_e) = -I$. There are three distinct cases.

a) If

$$s = (1 - \lambda)^2 + \lambda - \frac{3}{a\epsilon} < 0, \tag{3.7}$$

$\Phi(u)$ is decreasing, thus there exists a unique equilibrium for all values of I .

b) When $s = 0$, Φ has an inflection point at $u = \frac{1+\lambda}{3}$. The 3-dimensional set $s = 0, I = \Phi(\frac{1+\lambda}{3})$ consists of saddle-node bifurcation points. $\Phi(u)$ is decreasing, and there exists a unique equilibrium for all values of I .

c) If $s > 0$, $\Phi(u)$ has a maximum $I_M = \Phi(\frac{1+\lambda+\sqrt{s}}{3})$ and a minimum $I_m = \Phi(\frac{1+\lambda-\sqrt{s}}{3})$. Depending on the relation between I_M, I_m and I there can be 1, 2 or 3 equilibria. If $I_M < -I$ or if $I_m > -I$ there is only one equilibrium, if $I_m < -I < I_M$, there are three equilibria, while $I = -I_M$ and $I = -I_m$ are saddle-node bifurcation values of the parameter I .

3.2.2. Single Equilibrium Point: Stable, Unstable and Supercritical Hopf Bifurcation

If only one equilibrium, $E_0 = (u_0, w_0)$ exists, unlike $(0,0)$ for the $I = 0$ case, it can be either stable or unstable. The considerations in the previous section show that if (u_0, w_0) is a unique equilibrium and if $s \neq 0$, then $\Phi'(u_0) = \epsilon g'(u_0) - \frac{1}{a} < 0$. If $s = 0$, then $\Phi'(u_0) \leq 0$.

Further, Proposition 2.1 tells us that if $\epsilon g'(u_0) - \frac{1}{a} < 0$, then E_0 is asymptotically stable if

$$\epsilon g'(u_0) < a. \tag{3.8}$$

Thus, if E_0 is unique, it is asymptotically stable if (3.8) holds with the exception of the case when $s = 0$ and $I = -\Phi(\frac{1+\lambda}{3})$. It is unstable if $\epsilon g'(u_0) > a$. In this case a stable limit cycle exists, which follows from Poincaré-Bendixon's theorem. Because the exchange of stability is achieved via Hopf bifurcation (see 3.1) the stable cycle appears as a result of a supercritical one when $\epsilon g'(u_0) = a$.

We can combine these observations and the results from the previous section to obtain the following

Proposition 3.4. *If $s < 0$ or if $s \geq 0$ and either $I < -\Phi(\frac{1+\lambda+\sqrt{s}}{3})$ or $I > -\Phi(\frac{1+\lambda-\sqrt{s}}{3})$ hold, then the unique equilibrium $E_0 = (u_0, w_0)$ is asymptotically stable if either $a > 1$ or $\varepsilon g'(u_0) < a \leq 1$ and unstable if $a < \varepsilon g'(u_0) \leq 1$. In the last case, a stable periodic orbit exists around E_0 .*

When E_0 is unique and stable, there are cases in which we can prove that it is globally stable by using the Lyapunov functional from section 2.

Let us examine a numerical example with $a=0.06$, $\varepsilon = 14$, $\lambda = 0.5$ and vary I from 4 to 13 (Figure 3). There is a unique equilibrium for all these parameter values and two Hopf bifurcations take place. For $I < 4.2$ the unique equilibrium is stable and loses stability near this value. A supercritical Hopf bifurcation leads to the appearance of a limit cycle, whose amplitude increases initially with increase in I and later decreases again until a second Hopf bifurcation takes place at approximately $I = 12.43$, and the equilibrium becomes stable again. The supercriticality of the Hopf bifurcations is also supported by calculating the value of G_4 (see Appendix B) which is the same negative value in both cases, $G_4 = -6.11724$.

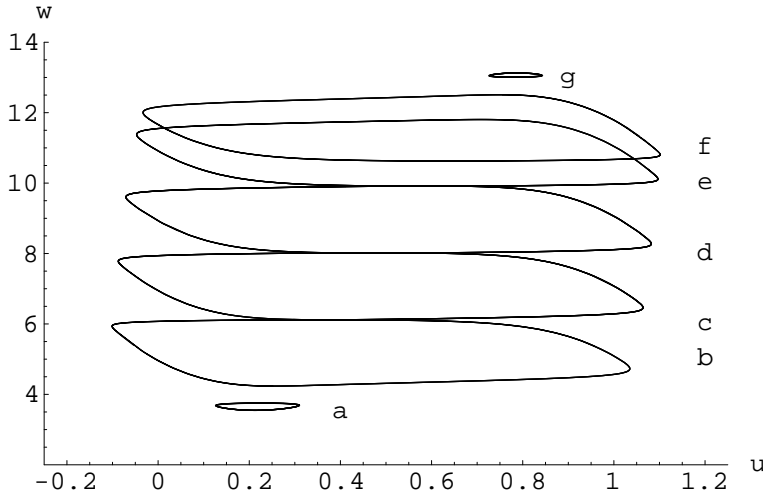


Figure 3: A limit cycle appears through Hopf bifurcation, moves upward and disappears through another Hopf bifurcation.
 $a = 0.06$, $\lambda = 0.5$, $\varepsilon = 14$.
(a) $I=4.26$, (b) $I=5$, (c) $I=7$, (d) $I=9$, (e) $I=11$, (f) $I=11.75$, (g) $I=12.42$

3.2.3. More Than One Equilibrium: Subcritical Hopf bifurcations

Keeping a, λ, ε fixed, the values $I = I_M$ and $I = I_m$ are equilibrium saddle-node bifurcation points, as noted in Section 3.2.1. These bifurcations occur when the slopes of the nullclines are the same, i.e. when $\varepsilon g'(u_e) = 1/a$. Similarly to the case when $I = 0$, these points are B-T bifurcation points if $a = 1$.

Suppose that (3.6) has three positive solutions: $E_0 = (u_0, w_0)$, $E_1 = (u_1, w_1)$, $E_2 = (u_2, w_2)$, where $u_0 < u_1 < u_2$. E_1 is always a saddle point, since $\varepsilon g'(u_1) > \frac{1}{a}$. For E_0 and E_2 it is easily seen that $\Phi'(u_i) = \varepsilon g'(u_i) - \frac{1}{a} < 0$, $i = 0, 2$. The equilibrium points E_0 and E_2 will be locally stable or repellers, depending on whether $\varepsilon g'(u_i)$ is less or greater than a .

(A) Obviously, if $a \geq 1$, the condition $\Phi'(u_i) < 0$, $i = 0$ or 2 implies stability of E_i .

(B) Let $a < 1$. Let us denote $\Psi(u) = \varepsilon g(u) - au$. Then E_i , $i = 0, 2$ is asymptotically stable if $\Psi'(u_i) < 0$ and unstable if $\Psi'(u_i) > 0$. Let $\alpha_M > \alpha_m$ be the roots of Φ' and $\gamma_M > \gamma_m$ be the roots of Ψ' . An easy calculation shows that $\alpha_M < \gamma_M$ and $\alpha_m > \gamma_m$. Since $\Phi'(u_i) < 0$, then $u_i < \alpha_m$ or $u_i > \alpha_M$. Therefore E_i is stable if $u_i < \gamma_m$ or $u_i > \gamma_M$ (see Figure 4). Thus the stability of E_0 and E_2 depends on the relative location of the roots of $\Phi(u) + I$ with respect to the roots of Ψ' when I varies.

Starting from a value of $I < -I_M$ and increasing I until $I > -I_m$, first only E_0 exists and it is stable if I is small enough (as in a) on Figure 4). When I is increased:

- α) E_0 becomes unstable;
- β) E_1 and E_2 appear via a saddle-node bifurcation, E_2 being unstable (as in Fig 4b);
- γ) E_2 becomes stable.

These three phenomena always occur but not always in this order.

δ) E_1 and E_0 disappear (as in Fig 4c).

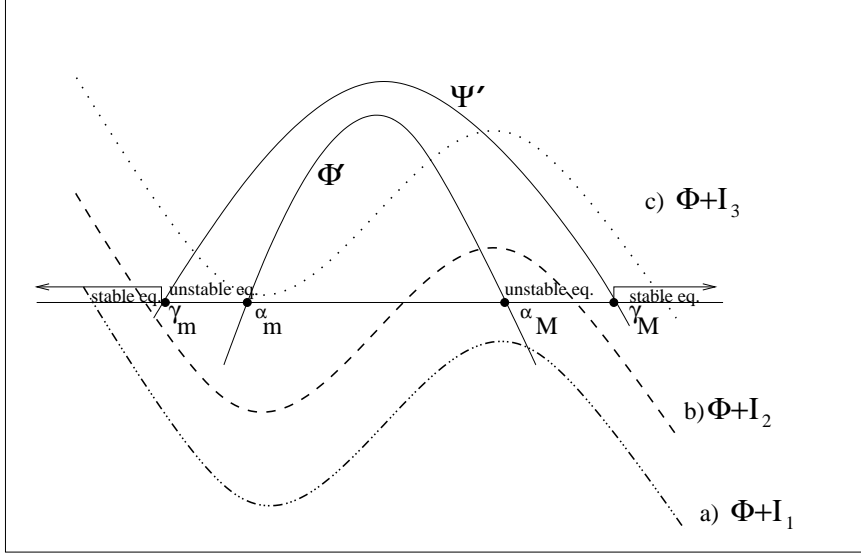


Figure 4: Equilibria of $\Phi + I$ are stable if located to the left of γ_m or to the right of γ_M and unstable if located between γ_m, α_m or α_M, γ_M . See text for more detail.

Eight different scenarios are possible which can be described in the following way. Let us denote by $E_i^q, i = 0, 2, q = s, u$ the equilibria $E_i, i = 0, 2$ in the cases when they are stable ($q = s$) or unstable ($q = u$). Then the 8 scenarios can be described as

$$\begin{aligned}
 (i) & E_0^s \rightarrow \{E_0^s, E_2^u\} \rightarrow \{E_0^u, E_2^u\} \rightarrow \{E_0^u, E_2^s\} \rightarrow E_2^s; \\
 (ii) & E_0^s \rightarrow E_0^u \rightarrow \{E_0^u, E_2^u\} \rightarrow E_2^u \rightarrow E_2^s; \\
 (iii) & E_0^s \rightarrow \{E_0^s, E_2^u\} \rightarrow \{E_0^s, E_2^s\} \rightarrow \{E_0^u, E_2^s\} \rightarrow E_2^s; \\
 (iv) & E_0^s \rightarrow \{E_0^s, E_2^u\} \rightarrow \{E_0^u, E_2^s\} \rightarrow E_2^s; \\
 (v) & E_0^s \rightarrow \{E_0^u, E_2^u\} \rightarrow \{E_0^u, E_2^s\} \rightarrow E_2^s; \\
 (vi) & E_0^s \rightarrow E_0^u \rightarrow \{E_0^u, E_2^u\} \rightarrow \{E_0^u, E_2^s\} \rightarrow E_2^s; \\
 (vii) & E_0^s \rightarrow \{E_0^s, E_2^u\} \rightarrow \{E_0^u, E_2^u\} \rightarrow E_2^u \rightarrow E_2^s; \\
 (viii) & E_0^s \rightarrow \{E_0^s, E_2^u\} \rightarrow \{E_0^u, E_2^u\} \rightarrow E_2^s.
 \end{aligned} \tag{3.9}$$

The notation $\{E_0^q, E_2^p\}, q, p = s, u$ means that both E_0 and E_2 exist, while E_i^q is used if only one equilibrium exists. E_1 is not included in the scheme to shorten notations. E_1 is present whenever both E_0 and E_2 are present and is always a saddle.

The 8 scenarios correspond to 8 bifurcation curves.

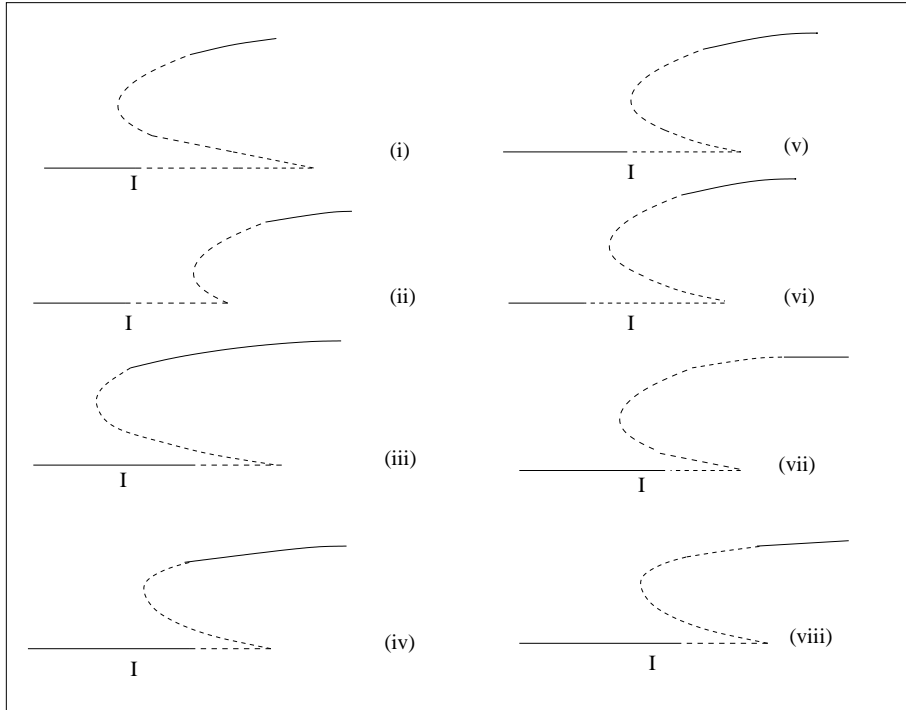


Figure 5: Eight possible bifurcation curves. See text.

The exchanges of stability are always accomplished via Hopf bifurcations. Since each of the scenarios involves 2 stability exchanges, which may be accomplished either via supercritical or subcritical Hopf bifurcation, it follows that the number of potential qualitatively different sequences of events is at least 32.

However, the appearance and disappearance of periodic orbits, not originating via Hopf bifurcations (possibly via homoclinic orbit of the saddle E_1 bifurcations) may make this number bigger.

We will not attempt to represent all the possible sequences of events that occur when I increases from $-\infty$ to $+\infty$. We shall illustrate the statement in the previous paragraph by presenting the results of a numerical computation of an example. It demonstrates the occurrence of several consecutive local and global bifurcation events when increasing the value of I , including saddle-node bifurcations of equilibria and of periodic orbits, subcritical Hopf bifurcations, homoclinic bifurcations, and a homoclinic orbit to a saddle converting to a heteroclinic one and vice versa.

Example 1. In this example $\varepsilon = 13.4$, $a = 0.3$, $\lambda = 0.0005$.

We describe the numerical experiment for increasing values of I . The calculations were carried out repeatedly with 3 different types of software. The results presented here are obtained using the package DVODE (Lawrence Livermore National Laboratory, [3]).

For small enough I the stable equilibrium E_0 is a global attractor. E_1 and E_2 appear via a saddle-node bifurcation but E_0 continues to be globally stable for small positive values of I attracting all solutions except E_1, E_2 and the stable manifold to E_1 . There exists no periodic solution. This is illustrated for $I = 0$ on Fig 6a.

When I is approximately 0.0258541, the numerical calculations surprisingly show that a stable and an unstable periodic orbit have appeared, seemingly simultaneously. One could suspect that a saddle-node bifurcation of periodic solutions has occurred, but this is not the case, because the bigger orbit is stable and surrounds all equilibria and the smaller one surrounds only E_0 and is unstable. E_0 attracts all solutions starting inside the unstable periodic orbit. E_2 is unstable in this case and all solutions starting outside of the unstable periodic orbit are attracted by the stable one. This is illustrated on Fig. 6b. (S)

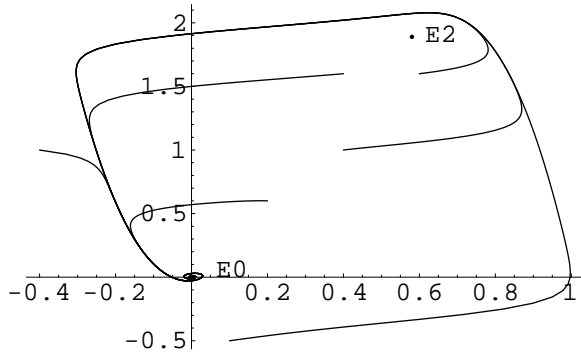


Figure 6a: $I=0$. E_0 attracts all solutions with the exception of the other two equilibria and the stable manifold to E_1 .

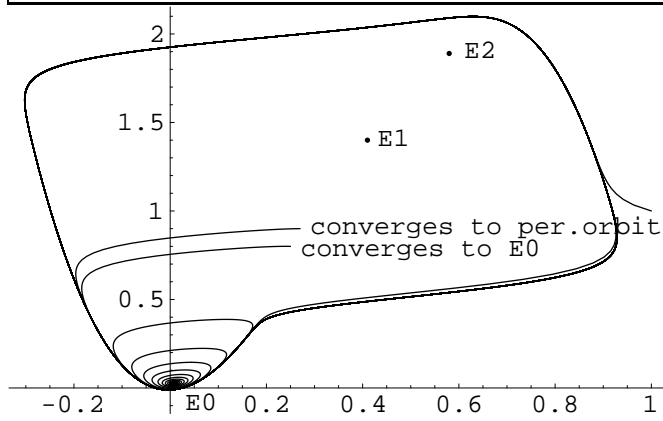


Figure 6b: $I=0.0258541$. The solution starting at $(0.27,0.9)$ converges to the stable periodic orbit, as does the depicted solution started at $(1,1)$. The solution starting at $(0.25,0.77)$ converges to the equilibrium E_0 . An unstable orbit exists that separates the solutions converging to E_0 and the solutions converging to the stable large orbit.

To understand this phenomenon, we conducted more accurate calculations. They showed that when I is slightly smaller ($I \approx 0.025854050872$), the solutions starting in a close proximity of E_2 are attracted by E_0 while the large periodic orbit also exists and attracts the solutions outside of it and in a certain region inside it to the right of E_0, E_1, E_2 line. This is illustrated on Figure 6c.

For values of I very close to but smaller than the above value the stable periodic solution does not exist. To get some insight, we calculated numerically the quantity

$$f = e^{\int_0^T [\varepsilon g'(p_I(s)) - a] ds}$$

where $p_I(s)$ is the numerically computed periodic solution, for several consecutive values of I between $I^* = 0.025854051$ and $I^{**} = 0.025854050872$. The quantity f is equal to the second Floquet multiplier (the first is 1) of $p_I(s)$. For these values of I , $f < 1$ and it increases fast, approaching 1, when I decreases. For example for $I = 0.025854051$, $f \approx e^{-18.36}$, for $I = 0.0258540509$, $f \approx e^{-10.04}$, for $I = 0.025854050872$, $f \approx e^{-0.575}$. We conclude that at a value I smaller than, but very close to $I^{**} = 0.025854050872$ the periodic solution becomes unstable. This loss of stability is accompanied by the coalescence of the stable periodic solution with an unstable one [5], p. 492.

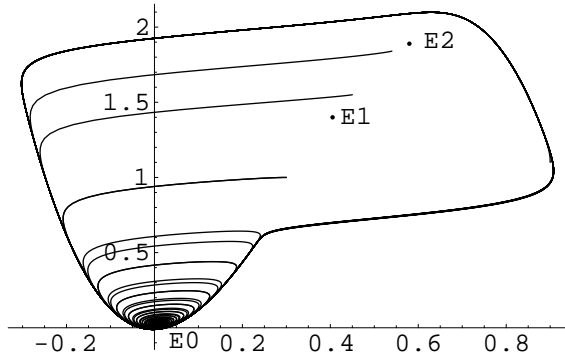


Figure 6c: $I = 0.025854050872$. All depicted solutions starting to the left of the equilibria converge to E_0 . See text for further explanation.

Further we present a possible reconstruction of the series of bifurcation events for values of I between I^* and I^{**} . A part of it was proposed by one of the referees and complemented by the first author. The basic player in all events is one of the stable manifolds of the saddle E_1 and specifically, its end at $-\infty$.

Starting with values of I larger than I^* and *decreasing* I , first an unstable (small and surrounding E_0) and stable (large) periodic orbits exist, as represented on Fig. 7I. One of the stable manifolds to E_1 is a heteroclinic orbit starting at $-\infty$ from the "small" periodic orbit. We shall refer to it as M_1 . The other manifold (M_2) is a heteroclinic orbit connecting E_2 and E_1 . While further decreasing I , the small periodic orbit and M_1 approach each other (Figure 7J) and coalesce into a homoclinic orbit of the saddle - i.e. now the $-\infty$ end of M_1 is at E_1 (Figure 7K). The homoclinic orbit is structurally unstable and converts into a heteroclinic one starting at $-\infty$ from E_2 (Fig. 7L), which gradually expands.

For slightly smaller I both stable manifolds to E_1 continue to be heteroclinic orbits (Figure 7L, M), surrounding the basin of attraction of E_0 . The numerical calculations fail to reveal what exactly happens further but it can be conjectured that the "big" heteroclinic orbit swells (Figure 7M) until it converts again to a homoclinic orbit Γ , i.e. the $-\infty$ end of M_1 is now at E_1 again (Figure 7N). The homoclinic orbit exists only at the point of bifurcation and disappears for smaller I to form an unstable "large" periodic orbit containing now all equilibria and located inside the stable periodic orbit (Fig. 7O). These two periodic orbits later on coalesce and disappear simultaneously (Fig. 7P).

Note that the events between the disappearance of the "small" and the "large" unstable periodic orbits happen very fast, i.e. in a very narrow range of values of I (an interval of magnitude 10^{-7} !). This is the reason why these events are hardly detectable via computations and why it originally seemed that the stable periodic solution disappears simultaneously with the "small" unstable periodic one.

The hypothetical scenario described above is the most probable one, as it is supported by numerical calculations. Another possible route we considered is the one in which the homoclinic orbit Γ (figure 7N) coalesces with the stable periodic solution. This would have been possible only if E_1 and the "angular" point A (Fig. 7N) of the stable orbit coalesce at the bifurcation value. Our numerical calculations show that this is not the case. When I approaches the bifurcation value, E_1 and A stay apart at almost the same distance.

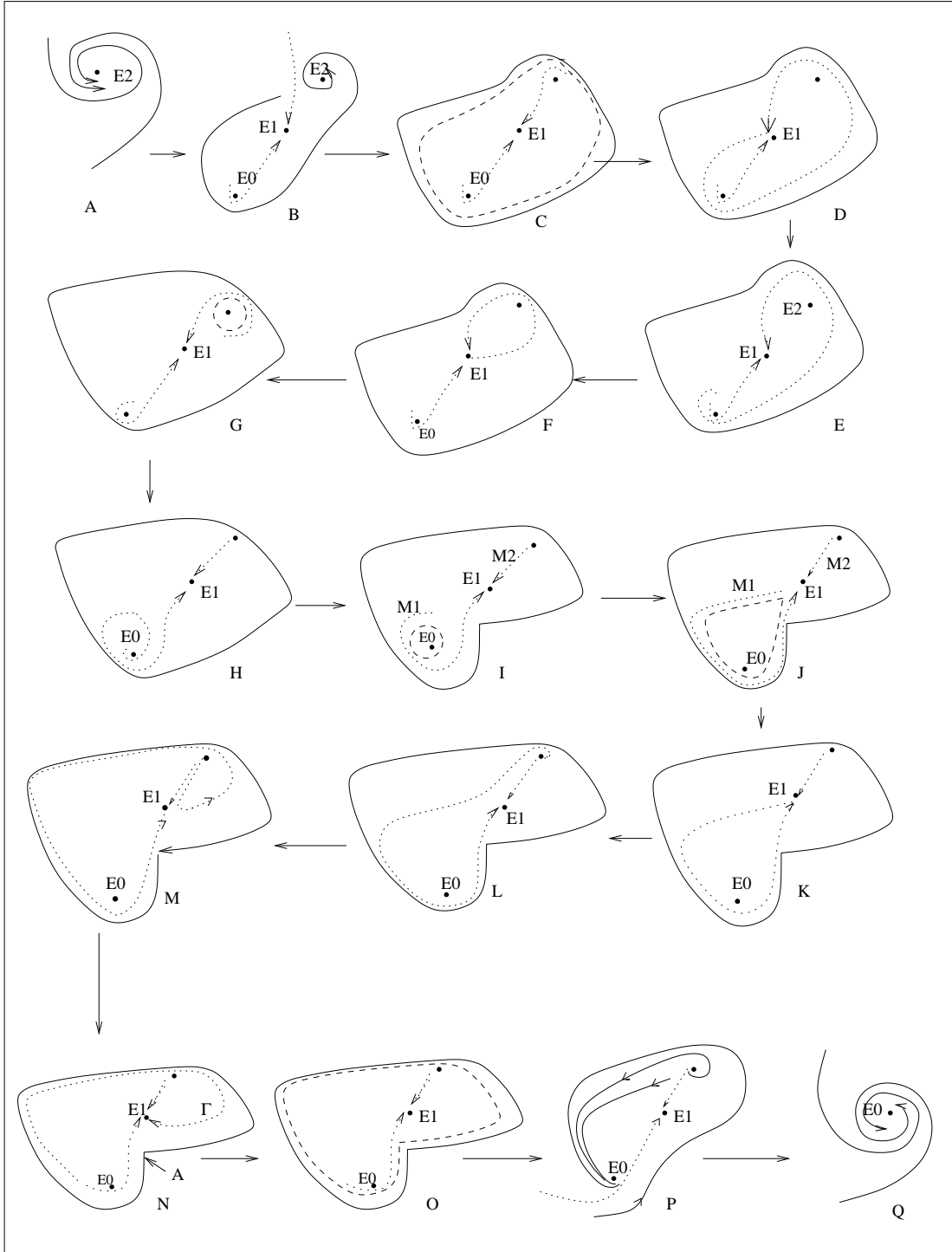


Figure 7: A full sequence of events corresponding to Example 1. A-Q plots are represented in decreasing order of I . Dashed lines correspond to unstable periodic orbits; solid lines - to stable periodic solutions and solution trajectories; dotted lines - to stable manifolds to the saddle. The shape of the limit cycle as depicted is only representative and does not correspond exactly to the actual one in all of the cases.

Additionally, the saddle quantity, [7], is positive:

$$\sigma = \varepsilon g'(u_1) - a > \frac{1}{a} - a = 1/0.3 - 0.3 > 0.$$

This indicates that the homoclinic orbit of the saddle appeared as a result of a bifurcation of an *unstable* periodic solution. These calculations and the loss of stability of the limit cycle make us believe in the validity of the proposed events.

Note that in this case the bifurcating unstable periodic solution is *outside* the homoclinic orbit - a non typical situation compared to the usually discussed in the literature ones ([7, 6]).

After this necessary “roll-back” we continue from the point (S) (just before Figure 6). *Increasing* I from 0.0258541, we observe numerically that E_0 loses stability and the remaining attractor is the large periodic orbit (Fig. 7H). At approximately $I = 0.2$, E_2 finally becomes stable (Fig. 7G). This is accomplished by a subcritical Hopf bifurcation. An unstable periodic solution appears when E_2 gains stability. The limit cycle still exists and all solutions starting out of the unstable periodic solution approach it. E_2 is stable for all values of I greater than 0.2. Further, when I is approximately equal to 0.2138, the small periodic solution disappears coalescing with the homoclinic orbit of the saddle as had happened (as described above) with the previously existing unstable periodic solution (Fig. 7F). In a manner completely similar to the steps illustrated on Figures 7M-O, the large periodic solution disappears next and finally, as I increases, the equilibrium points E_0 and E_1 approach each other and disappear in a saddle-node bifurcation, leaving E_2 the only attractor.

The sequence of events depicted on Figure 7 is in agreement with the bifurcation diagram on Figure 5(i). Obviously the same bifurcation diagram may correspond to different sequences of bifurcation events.

4 FH-N equations with periodic forcing

Consider FH-N equations with periodic forcing:

$$\begin{aligned}\dot{u} &= \varepsilon u(u - \lambda)(1 - u) - w + F(t), \\ \dot{w} &= u - aw,\end{aligned}\tag{4.1}$$

where $F(t)$ is a periodic forcing term with period T .

If we set $x = w$, $y = u - aw$, then

$$\dot{x} = y, \quad \dot{y} = -yf(x, y) - g_1(x) + F(t),$$

where f and g_1 are defined as in Section 2, $u_e = 0$. This is the Cauchy normal form of the second order equation:

$$\ddot{x} + f(x, \dot{x})\dot{x} + g_1(x) = F(t).$$

According to [5], pp. 171-178, if there are constants $\tilde{a}, m, M > 0$ such that:

(i) for $|x| \geq \tilde{a}, |y| \geq \tilde{a}, f(x, y) > m$,

(ii) for $(x, y) \in \mathbb{R}^2, f(x, y) > -M$,

(iii) for $|x| \geq \tilde{a}$, there holds $xg_1(x) > 0$,

(iv) the function $g_1(x)$ is monotone increasing in $(-\infty, -\tilde{a})$ and (\tilde{a}, ∞) ,

(v) $|g_1(x)| \rightarrow \infty$ as $|x| \rightarrow \infty$,

(vi) $g_1(x)/G(x) \rightarrow 0$ as $|x| \rightarrow \infty$, where $G(x) = \int_0^x g_1(u)du$,

then the system has a non constant periodic solution with the same period T of the forcing term.

Applying this result yields

Proposition 4.1. *If $F(t)$ is a T -periodic forcing, then (4.1) has a T -periodic solution.*

The proof is in Appendix A.

As a demonstration, we present an example with a FH-N system perturbed by the periodic “output” $u(t)$ of another similar system, i.e. the two systems are *coupled oscillators*.

Namely, we calculate numerically the solutions of the system

$$\begin{aligned}u' &= \varepsilon u(1 - u)(u - \lambda) - w + I \\ w' &= u - aw \\ u_1' &= \varepsilon_1 u_1(1 - u_1)(u_1 - \lambda_1) - w_1 + \theta u \\ w_1' &= u_1 - a_1 w_1,\end{aligned}\tag{4.2}$$

where $\varepsilon = 14$, $\varepsilon_1 = 13.4$, $a = 0.06$, $a_1 = 0.1$, $\lambda = 0.5$, $\lambda_1 = 0.005$, $I = 5$ and θ can take different values to enhance or weaken the forcing.

For $\theta = 0.75$ we find numerically that the whole system has a periodic attractor with a period equal to the forcing period.

Besides solutions with the same period T of the forcing function, it is possible to have solutions with a period, which is an integer multiple of T . For example, for $\theta = 0.05$, the forced system has a periodic attractor with a period twice as big as the forcing period.

It is worthwhile to remark that the last theorem proves that a periodic solution with the same period as that of the forcing exists (a phenomenon usually referred to as *phase locking*) no matter what the amplitude of the forcing is.

5 Acknowledgments

The authors thank two anonymous referees for detailed comments and criticisms which improved dramatically the quality of the paper and contributed enormously to the understanding of Example 1.

The first author acknowledges that her work on this version of paper was done under the auspices of the U.S. Department of Energy at the University of California Lawrence Livermore National Laboratory under contract No. W-7405-Eng-48.

References

- [1] D. Armbruster, [1997] "The (almost) complete dynamics of the FitzHugh Nagumo Equations", in: *Nonlinear Dynamics*, ed. A. Guran, (World Scientific), 89-102
- [2] D. Brown and P. Rothery, [1993] *Models in Biology: Mathematics, Statistics and Computing*, (J. Wiley & Sons)
- [3] P. N. Brown, G. D. Byrne, and A. C. Hindmarsh, [1989] "VODE, A Variable-Coefficient ODE Solver", *SIAM J. Sci. Stat. Comput.*, 10, pp. 1038-1051.
- [4] G. Dangelmayr and J. Guckenheimer, [1987] "On a four parameter family of planar vector fields", *Arch. Rat. Mech. Anal.* 97, 321-352
- [5] [1994] M. Farkas, *Periodic Motions*, (Springer-Verlag, Berlin)
- [6] [1997] J. Guckenheimer and P. Holmes *Nonlinear Oscillations, Dynamical Systems and Bifurcations of Vector Fields*, (Springer-Verlag, Berlin)
- [7] Yu. Kuznetsov, [1995] *Elements of Applied Bifurcation Theory*, (Springer-Verlag, Berlin)
- [8] J.D. Murray, 1989 *Mathematical Biology*, (Springer-Verlag, Berlin)
- [9] S. Rajasekar and M. Lakshmanan, [1988] "Period Doubling Route to Chaos for a BVP Oscillator with Periodic External Force", *J. Theor. Biol.*, 133, 473-477
- [10] S. Rajasekar and M. Lakshmanan, [1988] "Period Doubling Bifurcations, Chaos, Phase Locking and Devil's Staircase in a BVP oscillator", *Physica D*, 32, 146-152
- [11] S. Sato and S. Doi, [1992] "Response Characteristics of the BVP Neuron Model to Periodic Pulse Input", *Mathematical Biosciences*, 112, pp. 243-259
- [12] S. H. Strogatz, [1994] *Nonlinear Dynamics and Chaos*, (Perseus Books, Reeding, Massachusetts)

Appendix A.

Proof of Proposition 3.2. Consider the functional $V(u, w)$ defined by (2.1). For the (0,0) equilibrium we have

$$b_2 = \lambda + 1, b_1 = -\lambda.$$

We shall show that if (3.2) holds, i.e. if (0,0) is a unique equilibrium, then $G(w) \geq 0, \forall w$.

$G(w)$ is a polynomial of degree 4 in w , which has two repeated roots at the origin, i.e. $G(w)$ has a local extremum at 0. We explore the existence of other extrema.

$$G'(w) = 0 \Leftrightarrow g_1(w) = 0 \text{ (see 2.2).}$$

But

$$g_1(w) = -\varepsilon[g'(0)aw + \frac{1}{2}g''(0)(aw)^2 + \frac{1}{6}g'''(0)(aw)^3] + w$$

(see the definition of g_1 in Section 2.2). Since the last expression in the brackets is a part of a Taylor expansion of $g(aw)$ at 0, we get,

$$g_1(w) = -\varepsilon[g(aw) - g(0)] + w = -\varepsilon g(aw) + \frac{1}{a}aw.$$

Therefore,

$$G'(w) = 0 \Leftrightarrow \varepsilon g(aw) = \frac{1}{a}aw.$$

So, a value w_m is an extremum of G if and only if it satisfies $g(aw_m) = \frac{1}{a}aw_m$, which is true if and only if (aw_m, w_m) is an equilibrium solution. However, it was assumed that the only equilibrium is (0,0). It follows that the only extremum of G is at 0 and it is a minimum (as $G''(0) = 1 + \lambda\varepsilon a > 0$).

Thus, in the case of an unique equilibrium, $G(w)$ is positive everywhere, except at the origin, where it is zero. So, consequently, $V(u, w)$ is positive everywhere, except at the origin. This is true iff the value T from Section 2.2 is positive: $T > 0$ (Proposition 2.2, a)).

Further, for the value S defined in the beginning of Section 2.2, $S < 0$ is equivalent to

$$(1 - \lambda)^2 + \lambda - 3\frac{a}{\varepsilon} < 0, \quad (5.1)$$

which is equivalent to (3.3). Therefore, in the considered case, $T > 0, S < 0$, i.e. all conditions of Proposition 2.2 are fulfilled and thus (0,0) is a globally asymptotically stable equilibrium of (1.1). \square

Proof of Proposition 4.1

The existence of a constant positive value M is easy to establish since $f(x, y)$ has a minimum at $x = (\lambda + 1)/(3a), y = 0$ at which point f has the value $-\varepsilon(\lambda^2 - \lambda + 1)/3 - a$.

Set $M = |\varepsilon(\lambda^2 - \lambda + 1)/3 - a|$.

Further, if $\zeta \geq 0$ is large enough, the curve $\mathcal{E} : f(x, y) = \zeta$ exists and is an ellipse (compare with Section 2). Take a square $\mathcal{Q} = \{|x| < a_1, |y| < a_1\}$, containing \mathcal{E} and set $m = \zeta$.

Next, $xg_1(x)$ is a fourth degree polynomial, where the highest power in x has a positive coefficient. Therefore, for some a_2 , $xg_1(x) > 0$ if $x > a_2 > 0$.

Further, since $g_1(x)$ is a third degree polynomial, there is a a_3 , such that $g_1(x)$ is monotone increasing if $|x| > a_3$.

Set $\tilde{a} = \max(a_1, a_2, a_3)$. Then (i), (iii) and (iv) hold.

Finally, (v) and (vi) are immediate. This concludes the proof. \square

Appendix B. Stability of the periodic solutions arising through Hopf bifurcation

Suppose $\varepsilon g'(u_e) = a$. This is the condition for occurrence of Hopf bifurcation for system (1.1). Shift the equilibrium point (u_e, w_e) to the origin by the transformation $\tilde{u} = u - u_e, \tilde{w} = w - w_e$. Then make the transformation $\tilde{x} = a\tilde{u} + \tilde{w}, \tilde{y} = (1 + a^2)\tilde{u} - 2a\tilde{w}$.

The equations transform 1.1 to:

$$\begin{aligned} \dot{\tilde{x}} &= \tilde{y} + \varepsilon b_2 \left(\frac{2a\tilde{x} + \tilde{y}}{3a^2 + 1} \right)^2 - a\varepsilon \left(\frac{2a\tilde{x} + \tilde{y}}{3a^2 + 1} \right)^3, \\ \dot{\tilde{y}} &= -(1 - a^2)\tilde{x} + \varepsilon b_2(1 + a^2) \left(\frac{2a\tilde{x} + \tilde{y}}{3a^2 + 1} \right)^2 - \varepsilon(1 + a^2) \left(\frac{2a\tilde{x} + \tilde{y}}{3a^2 + 1} \right)^3, \end{aligned}$$

where $b_2 = g''(u_e)/2$.

If we set $\tau = \sqrt{1 - a^2}t$, $x = \sqrt{1 - a^2}\tilde{x}$, $y = \tilde{y}$ and $\dot{}$ stands for differentiation with respect to τ , then the equations can be written as:

$$\begin{aligned}\dot{x} &= y + a_0(p_1x + p_2y)^2 + a_1(p_1x + p_2y)^3, \\ \dot{y} &= -x + c_0(p_1x + p_2y)^2 + c_1(p_1x + p_2y)^3,\end{aligned}$$

where

$$\begin{aligned}a_0 &= ab_2\varepsilon, & a_1 &= -a\varepsilon, \\ p_1 &= \frac{2a}{\sqrt{1 - a^2}(3a^2 + 1)}, & p_2 &= \frac{1}{3a^2 + 1}, \\ c_0 &= \frac{1 + a^2}{\sqrt{1 - a^2}}\varepsilon b_2, & c_1 &= -\frac{1 + a^2}{\sqrt{1 - a^2}}\varepsilon.\end{aligned}$$

Following the Andronov- Hopf Bifurcation Theorem ([5], p.415-434), we look for a Lyapunov function of the form :

$$F(x, y) = x^2 + y^2 + \sum_{i=3}^m F_i(x, y),$$

where F_i is a homogeneous polynomial of degree i . Using

$F_3 = \alpha_0x^3 + \alpha_1x^2y + \alpha_2xy^2 + \alpha_3y^3$ and $F_4 = \beta_0x^4 + \beta_1x^3y + \beta_2x^2y^2 + \beta_3xy^3 + \beta_4y^4$, we choose the constants suitably, so that

$$\dot{F}(x, y) = G_4(x^2 + y^2)^2 + o((x^2 + y^2)^2).$$

This is done by choosing:

$$\begin{aligned}\alpha_0 &= -2(2a_0p_1p_2 + c_0p_1^2 + 2c_0p_2^2)/3, & \alpha_1 &= 2a_0p_1^2, \\ \alpha_2 &= -2c_0p_2^2, & \alpha_3 &= 2(2c_0p_1p_2 + a_0p_2^2 + 2a_0p_1^2)/3.\end{aligned}$$

β_1, β_3 are chosen so that they satisfy the two linear algebraic equations:

$$\begin{aligned}\beta_1 + \beta_3 &= 2a_1p_1^3 - 2c_1p_2^3 + 3a_0\alpha_0p_1^2 + c_0\alpha_1p_1^2 - a_0\alpha_2p_2^2 - 3c_0\alpha_3p_2^2, \\ 5\beta_1 - 3\beta_3 &= -6a_1p_1p_2^2 + 4a_1p_1^3 - 6c_1p_1^2p_2 + 3a_0\alpha_0(2p_1^2 - p_2^2) - 4a_0\alpha_1p_1p_2 + \\ & c_0\alpha_1(2p_1^2 - p_2^2) - a_0\alpha_2p_1^2 - 4c_0\alpha_2p_1p_2 - 3c_0\alpha_3p_1^2.\end{aligned}$$

G_4 is then given by :

$$G_4 = 2a_1p_1^3 + 3a_0\alpha_0p_1^2 + c_0\alpha_1p_1^2 - \beta_1.$$

Using this formula, we calculate G_4 in each separate case. If $G_4 < 0$, the periodic solution emerging through Hopf bifurcation is stable, i.e. the bifurcation is supercritical. If $G_4 > 0$, the periodic solution is unstable, i.e. the bifurcation is subcritical.

Email of authors:

kostova@llnl.gov
renrav@math.iisc.ernet.in
schonbek@math.ucsc.edu

Approved for public release; further dissemination unlimited

University of California
Lawrence Livermore National Laboratory
Technical Information Department
Livermore, CA 94551

